

computationally much harder. Finding an assignment that falsifies the minimum number of clauses is like finding the ground state in a spin glass phase and does not reduce to a single search on the directed graph of (14). For 2-SAT, in fact, finding such "ground states" is NP-hard (13). Therefore, if both diverging correlations (diverging in size if no lengths are defined) and a "spin glass" phase occur, we expect search to be exponentially difficult.

REFERENCES AND NOTES

1. P. Erdős and A. Rényi, *Publ. Math. Inst. Hung. Acad. Sci.* **5**, 17 (1960).
2. B. Bollobás, *Random Graphs* (Academic Press, London, 1985); J. Spencer, *Ten Lectures on the Probabilistic Method* (Society for Industrial and Applied Mathematics, Philadelphia, PA, 1987).
3. S. Janson, D. E. Knuth, T. Łuczak, B. Pittel, *Random Struct. Algorithms* **4**, 231 (1993).
4. D. Stauffer and A. Aharony, *Introduction to Percolation Theory* (Taylor and Francis, London, 1992).
5. D. Mitchell, B. Selman, H. J. Levesque, in *Proceedings of the 10th National Conference on Artificial Intelligence* (AAAI Press, Menlo Park, CA, 1992), p. 459; extended version in *Artif. Intell.*, in press.
6. V. Chvátal and B. Reed, in *Proceedings of the 33rd Annual Symposium on Foundations of Computer Science* (IEEE Society Press, Los Alamitos, CA, 1992), p. 620.
7. A. Goerdt, in *Proceedings of the 17th International Symposium on the Mathematical Foundation of Computer Science*, I. M. Havel and V. Koubek, Eds. (Springer-Verlag, Berlin, 1990), p. 264.
8. A. Z. Broder, A. M. Frieze, E. Uptal, in *Proceedings of the 4th Annual ACM-SIAM Symposium on Discrete Algorithms* (Society for Industrial and Applied Mathematics, Philadelphia, PA, 1993), p. 322.
9. J. M. Crawford and L. D. Auton, in *Proceedings of the 11th National Conference on Artificial Intelligence* (AAAI Press, Menlo Park, CA, 1993), p. 21.
10. T. Larrabee and Y. Tsujii, in *Proceedings of the AAAI Symposium on Artificial Intelligence and NP-Hard Problems* (1993), p. 112.
11. B. Selman, H. J. Levesque, D. Mitchell, in (5), p. 440.
12. A. P. Kamath *et al.*, *Ann. Oper. Res.* **25**, 43 (1990).
13. S. A. Cook, *Proceedings of the 3rd Annual ACM Symposium on Theory of Computing* (Association for Computing Machinery, New York, 1971), p. 151.
14. B. Aspvall, M. F. Plass, R. E. Tarjan, *Inf. Process. Lett.* **8**, 121 (1979).
15. P. Cheeseman, B. Kanefsky, W. M. Taylor, in *Proceedings of the 12th International Conference on Artificial Intelligence*, R. Reiter and J. Mylopoulos, Eds. (Morgan Kaufmann, San Mateo, CA, 1991), p. 331.
16. M. Mézard, G. Parisi, M. A. Virasoro, *Spin Glass Theory and Beyond* (World Scientific, Singapore, 1986).
17. S. Kirkpatrick and R. H. Swendsen, *Commun. ACM* **28**, 363 (1985).
18. M. N. Barber, in *Phase Transitions and Critical Phenomena*, C. Domb and J. L. Lebowitz, Eds. (Academic Press, London, 1983), vol. 8, p. 145.
19. M. Davis and H. Putnam, *J. Assoc. Comput. Mach.* **7**, 201 (1960).
20. O. Dubois, P. Andre, Y. Boufkhad, J. Carlier, in *Proceedings of the 2nd DIMACS Implementation Challenge* (American Mathematical Society, Providence, RI, in press).
21. S. Kirkpatrick, G. Gyögyi, N. Tishby, L. Troyansky, in *Advances in Neural Information Processing Systems*, vol. 6, J. Cowan, G. Tesaro, J. Alspector, Eds., in press; and unpublished results.
22. S. H. Clearwater, B. A. Huberman, T. Hogg, *Science* **254**, 1181 (1991).
23. Y. Fu, in *Lectures in the Sciences of Complexity*,

D. Stein, Ed. (Addison-Wesley, Reading, MA, 1989), p. 815.

24. This work was done during S.K.'s 1993 sabbatical at the Racah Institute of Physics and Center for Neural Computation, Hebrew University, Jerusalem, 91904 Israel. A portion of the work was carried out at the Salk Institute, with support from the McDonnell-Pew Foundation.

lem, 91904 Israel. A portion of the work was carried out at the Salk Institute, with support from the McDonnell-Pew Foundation.

30 November 1993; accepted 23 March 1994

Langmuir-Blodgett Films of a Functionalized Molecule with Cross-Sectional Mismatch Between Head and Tail

J. Garnæs, N. B. Larsen, T. Bjørnholm,* M. Jørgensen, K. Kjaer, J. Als-Nielsen, J. F. Jørgensen, J. A. Zasadzinski

A functionalized surfactant has been investigated as floating monolayers by synchrotron x-ray diffraction and as bilayers transferred to solid supports by the Langmuir-Blodgett technique through atomic force microscopy. The transfer process is accompanied by an increase of the unit cell area (about 17 percent) and by an increase of the average domain diameter of nanometer-scale domains (about three times). The unit cell area of the floating monolayer corresponds to close packing of the head groups and a noncharacteristic packing of the tilted alkyl chains. The larger unit cell area of the bilayer film is consistent with a particular ordered packing of the alkyl chains, leaving free space for the head groups.

As a means of organizing complex molecules, the Langmuir-Blodgett (LB) technique (1) has many potential applications within molecular electronics, nonlinear optics, and conducting thin films (Fig. 1). In this context, the structural properties of the LB films may have important consequences for applications; for example, the number of defects may limit electrical contact, while the degree of order and the sizes of domains may limit, for example, the conductivity. In addition, changes of these properties may occur when the floating monolayers are transferred to solid substrates. By the combination of x-ray diffraction (XRD) of floating monolayers with atomic force microscopy (AFM) of films transferred to solid supports, it is possible to reveal these features.

Because molecules with relatively large head groups, compared to alkyl chains, are often used in functionalized LB films (Fig. 1), the design of the functional organic molecules requires an understanding of the packing properties of molecules with a "cross-sectional mismatch" between head and tail groups. As an example of such a molecule, we present a structural study performed of both a floating monolayer and a bilayer transferred to a solid substrate.

J. Garnæs and J. F. Jørgensen, Danish Institute of Fundamental Metrology, Lundtoftevej 100, DK-2800 Lyngby, Denmark.

N. B. Larsen, T. Bjørnholm, M. Jørgensen, Centre for Interdisciplinary Studies of Molecular Interactions, Department of Chemistry, University of Copenhagen, Fruebjergvej 3, DK-2100 Copenhagen, Denmark. K. Kjaer and J. Als-Nielsen, Physics Department, Risø National Laboratory, DK-4000 Roskilde, Denmark. J. A. Zasadzinski, Department of Chemical and Nuclear Engineering, University of California, Santa Barbara, CA 93106, USA.

*To whom correspondence should be addressed.

The particular molecule in question is an electron acceptor, octadecylthio-1,4-benzoquinone (Fig. 1E), which forms nonlinear optical films when interfaced with electron donor molecules (2, 3).

Previous comparative studies of floating monolayers and transferred multilayers have focused on fatty acids and similar types of compounds that have head and tail groups of similar cross-sectional size. Such compounds have been extensively studied by XRD in situ at the water surface (4–9) and by AFM (10–13) and electron diffraction (14) as transferred multilayers. These studies have in many cases revealed highly

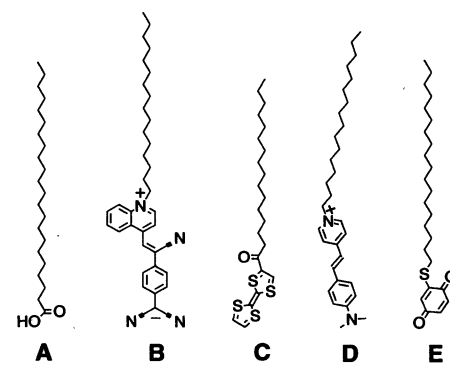


Fig. 1. Molecules used in LB films in different areas of research. (A) Fatty acids (26) have been the prototype for structural studies of LB films. Opposed to fatty acids, a large head group is common for electronically active molecules. The functionalized molecules given in this table have been used for (B) electrical rectification (27), (C) conduction/redox activity (28), (D) nonlinear optics (29), and (E) redox activity such as electron acceptor (2, 3, 20).

ordered structures extending for several micrometers in the films.

A study of the two-dimensional packing pattern of a floating monolayer of the acceptor was performed by synchrotron XRD (15). A solution of the acceptor in CHCl_3 was spread on a pure water surface followed by compression at a slow rate to a surface pressure of 20 mN/m (16), which is about one-half of the collapse pressure as well as the pressure used for transfer of films. This surface pressure was kept constant during the x-ray measurements. A beam of wavelength 0.1351 nm was incident slightly below the critical angle for total reflection. Detection of both the horizontal and vertical components of the diffracted beam was done by a vertically oriented position-sensitive detector (PSD).

Changes over time in the molecular ordering were investigated by performing the diffraction measurements in two steps. A fast scan of the horizontal angle with integration of all channels in the PSD for each angle was performed to probe the unit cell parameters, followed by a slower scan with individual PSD channels resolved to probe both the unit cell parameters and the conformation of the molecules. The results of the slow diffraction scan integrated over the PSD channels corresponding to each

peak are shown in Fig. 2A. Curve-fitting of the peaks of the slow scan gives d spacings of 0.553, 0.413, and 0.368 nm (domain diameters of 3.3, 3.0, and 3.6 nm for perfectly ordered domains) for the {10}, {01}, and {11} directions, respectively, to yield an oblique unit cell (Fig. 3A) (Table 1). For comparison, curve-fitting of the corresponding three peaks of the first (fast) scan gives d spacings of 0.549, 0.416, and 0.362 nm (domain diameters of 3.5, 3.3, and 8.6 nm). The difference in domain diameters for the two scans along the {11} direction indicates that some disordering takes place during the diffraction scans (about 4 hours), but without significant changes of the unit cell parameters.

Bragg rod scans (17) of each of the measured peaks integrated over the angular width of the peak are shown in Fig. 2B. The three Bragg rods were compared to a model that describes the diffracting part of each molecule as a long narrow cylinder (17). The fitting of the model parameters gives a cylinder of length 1.7 ± 0.2 nm tilting by $39^\circ \pm 2^\circ$ in a direction $31^\circ \pm 1^\circ$ away from the [10] direction toward the [1 $\bar{1}$] direction (Fig. 3A). The cylinder description fits approximately with the alkyl chain of all-trans length ≈ 2.2 nm, where we attribute the difference in length to a decrease in

order of the alkyl chain close to the head group or close to the film-air interface.

For comparison of the above results with transferred LB films, a bilayer of the acceptor was prepared. Bilayers of the acceptor deposited on silicon have been found to crystallize very easily (18). To prevent crystallization and thus retain the two-dimensional structure of the LB film, a bilayer of the acceptor was prepared on top of a bilayer of cadmium behenate deposited on a polished and cleaned hydrophobic silicon wafer (19, 12, 20). A study of the surface structure of the transferred film was performed with AFM (21). Imaging of the molecular order was done by measurement of the z deflection of the cantilever when the sample was scanned at constant height ("force mode"). Imaging of nanometer-scale topography, such as steps, was done by adjustment of the sample height to keep the cantilever deflection constant ("height mode"). A repulsive force less than 10 nN was used for imaging.

Images of the nanometer-scale topography of the bilayer of the acceptor showed flat and defect-free areas typically $>20 \mu\text{m}^2$ (Fig. 4a). When a force larger than 10 nN was used, holes could actively be formed in the LB film. From a height histogram (inset of Fig. 4a) and molecular resolved images (Fig. 4b) we could unambiguously identify the top layer, with a measured height of 4.5 ± 0.2 nm (20), as a bilayer of the acceptor and the bottom layer as a bilayer of cadmium behenate, where we used a value for the height of 6.04 nm from XRD (1).

Zooming in on the topmost acceptor layer revealed the molecular order (Fig. 4b), yielding unit cell parameters given in Table 1 and Fig. 3A. A scan area of 31 by 31 nm^2 where five domains with different orientations are present is shown in Fig. 4c.

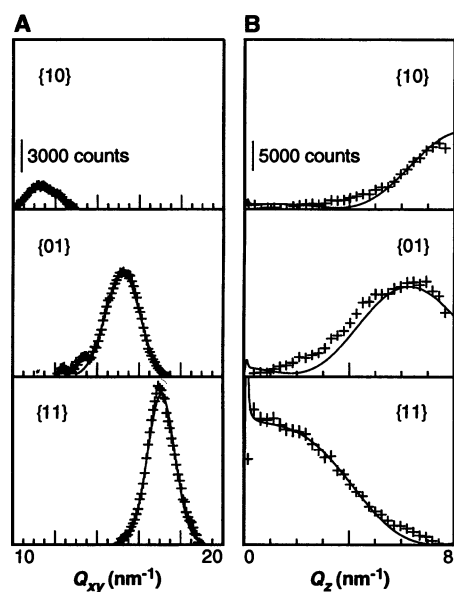


Fig. 2. Results of the slow grazing angle XRD scan for the three peaks measured (lattice indices are given above each graph). Measurements are given by crosses, and the solid lines are fitted curves. (A) The scattered intensity as a function of the horizontal component, Q_{xy} , of the scattering vector for each peak integrated over the channels of the PSD that make contributions to the peak. (B) The scattered intensity as a function of the vertical component, Q_z , of the scattering vector integrated over the horizontal scattering vectors of the corresponding peak in (A).

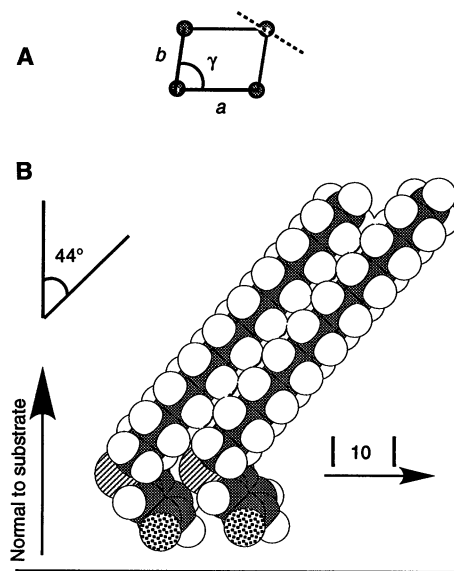


Fig. 3. (A) A schematic diagram of the one molecular oblique unit cell in the plane of the water surface or the bilayer substrate. The unit-cell parameters are given in Table 1. The dashed line shows the approximate orientation of the projection of the alkyl chain on the water subphase. The head-group orientation has not been determined in the experiments. (B) Space-filling model of two molecules of octadecylthio-1,4-benzoquinone arranged in the packing pattern $T[1\frac{1}{2}0]$ with bond lengths and angles obtained with the molecular mechanics program PC Model 4 (Serena Software, Bloomington, Indiana).

Table 1. Comparison of structural data for floating monolayers (surface pressure of 20 mN/m) and bilayer LB films (transfer pressure of 20 mN/m) of the acceptor. Unit cell dimensions refer to Fig. 3A.

Parameter	Floating monolayers	LB films
<i>Unit-cell dimensions</i>		
a (nm)	0.560 ± 0.005	0.587 ± 0.010
b (nm)	0.419 ± 0.005	0.456 ± 0.008
γ (degrees)	80 ± 1	82.3 ± 1
Area (nm^2)	0.231 ± 0.007	0.265 ± 0.008
<i>Other dimensions</i>		
Tilt angle of alkyl chains (degrees)	39 ± 2	
Thickness of bilayer (nm)	4.5 ± 0.2	
Domain diameter (nm)	3	10 to 20

Scan areas $>200 \text{ nm}^2$ on more than 15 places showed two or several domains with different orientations. From the images, we have estimated that $>90\%$ of the surface was covered by domains with a diameter of 10 to 20 nm. The widths of spots in the Fourier transformation have been analyzed, showing that the domains are perfectly ordered within experimental accuracy. A comparison of structural data for floating monolayers and LB films (Table 1) shows that the transfer of a bilayer of the acceptor results in a 17% expansion of the unit cell area. This expansion occurs along both crystallographic directions, rendering the angle of the oblique unit cell unchanged.

In crystals of the benzoquinone head group of the acceptor, the area of the group projected to the horizontal plane has been shown to be $\approx 0.23 \text{ nm}^2$ (22). In the pressurized films floating on water, this value corresponds to the observed area per molecule, indicating that the head groups are space-limiting and close-packed. To compensate for the discrepancy in cross-sectional area between the close-packed head groups ($\approx 0.23 \text{ nm}^2$) and close-packed alkyl chains ($\approx 0.185 \text{ nm}^2$), the chains must tilt. A simple space-filling argument based on the measured lattice parameters suggests a tilt angle of $\approx 37^\circ$, in agreement with experimental results. The possible tilted arrange-

ments of close-packed arrays of alkanes have been studied theoretically (22, 23), giving rise to a set of arrangements in fair agreement with measured crystal structures of undistorted alkanes (24, 25). On the basis of the deduced direction of the tilt relative to the unit cell vectors in floating monolayers of the acceptor, the packing of the alkyl chains does not fall into one of these characteristic arrangements.

Previous experience with AFM on fatty acids shows that imaging with molecular resolution is only possible when the alkyl chains are fixed in a rigid regular lattice (11, 12). Because the observation of perfectly ordered domains of the bilayer is possible with the AFM, we assume that the alkyl chains are fixed in such a lattice. If the lattice is to be space-filling with a molecular area of $\approx 0.27 \text{ nm}^2$, the tilt angle of the alkyl chains must be $\approx 46^\circ$. On the basis of the characteristic packing patterns for alkanes calculated by Kitaigorodskii (22, 23), we can calculate unit cell parameters for the packing pattern $T[1\frac{1}{2},0]$ shown in Fig. 3B of $a = 0.45$, $b = 0.56 \text{ nm}$, and $\gamma = 80^\circ$, with the alkyl chain tilting by 44° toward the next nearest neighbor. The agreement of these unit cell parameters with experimental results is good, making it a likely arrangement of the bilayer. Compared to the floating monolayer, this arrangement indi-

cates changes not only in the area per molecule but also in the tilt direction of the alkyl chains, allowing them to organize in a more stable arrangement.

The direct imaging of domains in the bilayer of the acceptor (Fig. 4c) provides information about the potential application of this molecule in functionalized LB films. For example, conduction in films incorporating the acceptor is likely limited by domain boundaries. Optical properties may also be influenced by the presence of highly ordered domains of submicrometer dimensions. On LB films of salts of fatty acids, the regular lattice structure of the untilted molecules is preserved as close as 1 nm from the boundaries (10). On the images of the acceptor, the domain boundaries are not sharp and consist of regions without order with a typical width of 2 to 5 nm. The disruption of the ordered packing is probably due to different tilt directions of neighboring domains. These disordered domain boundaries further reduce the possibility of making conducting films on the basis of the acceptor. The observed average domain diameter is significantly larger in the bilayer ($\approx 15 \text{ nm}$) than in the floating monolayer ($\approx 3 \text{ nm}$). This result suggests that the pressurized floating monolayer is in a strained state at the time of transfer because of the cross-sectional mismatch between head and tail. This strain is released upon transfer, allowing the alkyl chains to pack in a pattern typical for alkanes.

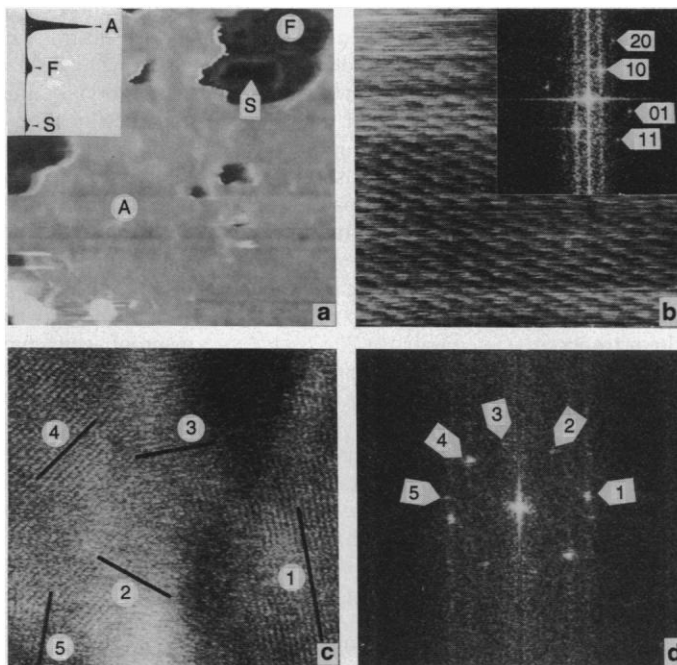
The nanometer-scale topography of the acceptor surface is similar to the topography found on the etched silicon substrate, which suggests that the surfaces of both the cadmium behenate and the acceptor follow the contours of the substrate. On a larger scale, Fig. 4a shows that the largest areas free of point defects are on the order of $20 \mu\text{m}^2$, which sets an upper limit for the size of electrical contact that can be made to a defect-free area.

These results show that the competition between packing of head groups and alkyl chains has important consequences for the microscopic structure of LB films and the size of ordered domains. Depending on the details of the application of the functionalized surfactant, these structural factors may be important, stressing the need for an accurate design of the molecules. For the evaluation of different concepts of molecular design for optimized LB films, the combination of synchrotron XRD and atomic force microscopy constitutes an efficient tool.

REFERENCES AND NOTES

1. G. G. Roberts, *Langmuir-Blodgett Films* (Plenum, New York, 1990).
2. T. Bjørnholm, T. Geisler, J. Larsen, M. Jørgensen, *Chem. Commun.* **11**, 815 (1992).
3. T. Bjørnholm *et al.*, *Synth. Met.* **57**, 3813 (1993).

Fig. 4. (a) AFM image ($8 \mu\text{m}$ by $8 \mu\text{m}$) of a bilayer of the acceptor deposited on a bilayer of cadmium behenate deposited on polished silicon. The surface of the acceptor (A), the cadmium behenate (F), and the silicon substrate (S) are indicated. The inset is a height histogram of a similar area. Areas marked with "A" indicate the height density due to the surface of the acceptor, "F" the cadmium behenate, and "S" the silicon substrate. (b) AFM image (14.1 nm by 14.1 nm) showing molecular resolution of the surface of the acceptor. The inset shows a Fourier transformation of the image.



The reciprocal lattice vectors are marked. The horizontal and vertical lines through the center and the strong spots are noise due to the raster scanning and the finite image size. Only the long repeat distance corresponding to (10) is clearly seen in the real-space image. (c) AFM image (31 nm by 31 nm) showing the molecular resolution of five domains with different crystallographic orientations. The domains are marked with numbers from 1 to 5 and lines along rows of molecules spaced by 0.59 nm are drawn in each domain. The boundaries and rows of molecules can be identified in the view of a grazing angle along the lines. (d) Fourier transformation of the image in (c). The arrows point toward the (10) spots caused by the five different domains. The other and weaker spots present in Fourier transformation in (b) are not seen on this larger scan area.

4. M. L. Schlossman *et al.*, *Phys. Rev. Lett.* **66**, 1599 (1991).
5. K. Kjaer *et al.*, *J. Phys. Chem.* **93**, 3200 (1989).
6. R. M. Kenn *et al.*, *J. Chem. Phys.* **95**, 2092 (1991).
7. D. Jacquemain *et al.*, *J. Am. Chem. Soc.* **113**, 7684 (1991).
8. B. Lin *et al.*, *Phys. Rev. Lett.* **111**, 191 (1990).
9. F. Leveiller *et al.*, *Science* **252**, 1532 (1991).
10. J. Garnaes, D. K. Schwartz, R. Viswanathan, J. A. N. Zasadzinski, *Nature* **357**, 54 (1992).
11. D. K. Schwartz, J. Garnaes, R. Viswanathan, J. A. N. Zasadzinski, *Science* **257**, 508 (1992).
12. D. K. Schwartz *et al.*, *Phys. Rev. E* **47**, 452 (1993).
13. J. Garnaes, D. K. Schwartz, R. Viswanathan, J. A. N. Zasadzinski, *Synth. Met.* **55-57**, 3795 (1993).
14. J. R. Peterson, R. Steith, H. Krug, I. Voight-Martin, *J. Phys.* **51**, 1003 (1990).
15. The floating monolayer was studied with the liquid surface diffractometer on wiggler beamline BW1 at HASYLAB, DESY, Hamburg, Germany. A beam of wavelength 0.1351 nm was incident on the surface at an angle $\alpha = 0.85\alpha_c$ to enhance surface sensitivity, where α_c is the critical angle for total external reflection, giving a footprint of 50 by 5 mm. The background level of scattering was reduced by the maintenance of a He atmosphere inside the trough. Detection was done by a vertically oriented PSD with 256 channels mounted behind a Soller collimator, giving a horizontal resolution (full width at half maximum) of 0.114 nm^{-1} and a vertical resolution of 0.050 nm^{-1} per channel.
16. The water phase was Millipore filtered water with resistivity $>18 \text{ M ohm} \cdot \text{cm}$ and thermostated at $20.0^\circ \pm 0.1^\circ \text{C}$. Chloroform was of analytical grade purchased from Merck (Rahway, NJ). The monolayer was compressed at a rate of 0.009 nm^2 per molecule per minute. After compression, the surface pressure was kept constant by the adjustment of the barrier position.
17. J. Als-Nielsen and K. Kjaer, in *The Proceedings of the NATO Advanced Study Institute, Phase Transitions in Soft Condensed Matter*, T. Riste and D. Sherrington, Eds. (Plenum, New York, 1989), pp. 113-137; K. Kjaer, *Physica B*, in press.
18. J. Garnaes, T. Bjørnholm, M. Jørgensen, J. A. N. Zasadzinski, *J. Vac. Sci. Technol.*, in press.
19. Spreading and compression were done in a manner similar to the procedure in the synchrotron study (15). The silicon wafer was cleaned in a solution of H_2O_2 and H_2SO_4 and then etched in hydrofluoric acid to make it hydrophobic. The LB films were transferred by the use of KSV-5000-3 (KSV Instruments, Helsinki) deposition equipment at a deposition speed of 1 mm/min. Cadmium behenate was transferred from a floating monolayer of behenic acid ($>99\%$, Aldrich) with a subphase containing $5 \times 10^{-4} \text{ M CdCl}_2$ (99.99%, Aldrich) and with the pH adjusted to 6.5. For both the cadmium behenate and the acceptor, the amount of film transferred was 1.0 ± 0.1 of a monolayer at both the downstroke and upstroke.
20. T. Bjørnholm *et al.*, *Synth. Met.* **57**, 3807 (1993).
21. For imaging, we used a Nanoscope III FM (Digital Instruments, Santa Barbara, CA) and microfabricated Si_3N_4 tips formed on cantilevers with a spring constant of 0.1 to 0.6 N/m. The x and y (horizontal) calibration was performed from 28 images of mica [absolute uncertainty 1.7% (12)]. The z calibration was calculated from bilayer step heights on LB films of fatty acids (13). We did not apply image processing or on-line filtering to any of the images of molecules. Unit-cell parameters were calculated from images of five domains recorded with two different tips.
22. A. I. Kitaigorodskii, *Organic Chemical Crystallography* (Consultant Bureau, New York, 1961).
23. ———, *Molecular Crystals and Molecules* (Academic Press, London, 1973).
24. S. Abrahamson, B. Dahlén, H. Löfgren, I. Pascher, *Prog. Chem. Fats Other Lipids* **16**, 125 (1978).
25. B. T. G. Liesner and G. Wegner, *Thin Solid Films* **68**, 77 (1980).
26. K. B. Blodgett, *J. Am. Chem. Soc.* **57**, 1007 (1935).
27. A. S. Maryin, J. R. Sambles, G. J. Ashwell, *Phys. Rev. Lett.* **70**, 218 (1993).

28. A. S. Dhindsa, M. R. Bryce, J. P. Lloyd, M. C. Petty, *Thin Solid Films* **165**, L97 (1988).
29. I. R. Girling *et al.*, *J. Opt. Soc. Am. B* **4**, 950 (1987).
30. We thank K. Bechgaard, K. Carneiro, T. Geisler, L. Nielsen, K. Schaumburg, and P. Sommer-Larsen for useful discussions; S. Munk for technical assistance; and HASYLAB at DESY, Hamburg, Ger-

many, for beam time. Supported by the Danish Materials Technology Development Program, the Danish Natural Science Research Council (grant 3.70.01-08/93), the U.S. Office of Naval Research (grant N00014-90-J-1551), and the NSF (grants CTS 9212290 and CTS 91-02719).

1 February 1994; accepted 4 April 1994

Evidence for Monophyly and Arthropod Affinity of Cambrian Giant Predators

Jun-yuan Chen, Lars Ramsköld,* Gui-qing Zhou

The Chinese Early Cambrian Chengjiang fauna includes three different anomalocaridids, a globally spread, extinct marine group including the largest known Cambrian animals. Anomalocaridids were active predators, and their presence implies that a complex ecosystem appeared abruptly in the earliest Phanerozoic. Complete specimens display several sets of characters shared only with some other exclusively Cambrian forms. This evidence indicates that anomalocaridids, *Opabinia*, and *Kerygmachela* form a monophyletic clade. Certain features indicate arthropod affinities of the clade, and for this group an unnamed (sub)phylum-level taxon within an arthropod (super)phylum is proposed.

The rapid diversification of animal life near the base of the Phanerozoic Eon is unparalleled in the history of life, but researchers are far from reaching a consensus on the origin of animal phyla or how they are related. This early radiation of the Metazoa produced perhaps all animal phyla extant today and some additional, extinct groups. In this report we discuss one such group, composed of large predators. Their presence in the Early Cambrian is important for the understanding of early metazoan evolution, trophic levels, and life habits. The diversity of the group implies that considerable evolution took place during a time interval even shorter (1) than previously suspected. This pattern parallels that of other Early Cambrian groups and is at the heart of two questions: the "Cambrian explosion" and the early evolution of the largest animal group on Earth, the arthropods.

Fossils usually preserve only hard or mineralized parts, and as most early metazoans lack such parts, the rare early Palaeozoic occurrences of soft tissue preservation are crucial for our knowledge of metazoan early evolution. For 75 years the Canadian Middle Cambrian Burgess Shale fauna provided most data on soft-bodied animals, but similar preservation is now known to be widespread in Cambrian rocks (2). An important site was discovered in 1984 (3) in Chengjiang, Yunnan, south China, and is approximately late Atdabanian (about 525 to 530 million years old). The Chengjiang

fauna (4) may have lived only 5 million years (1) after the "Cambrian explosion" began at the onset of the Tommotian age. The superb preservation and high diversity (5) (now close to 100 known species) equal those of the Burgess Shale fauna which is ~10 million years younger.

Mineralized parts in both metazoans, protists and cyanobacteria (6), as well as a diverse macrofauna producing varied trace fossils (7), appear abruptly close to the Precambrian-Cambrian boundary. This major diversification of life forms is known as the "Cambrian explosion." The biotic system appears to have quickly reached a level of complexity not far from that present in modern oceans. As today, suspension feeding and deposit feeding were the dominant means of primary consumption (8). As long as evidence to the contrary was lacking, macrophagous predators were thought to have evolved much later in the Cambrian. With the redescription of the Burgess Shale fauna, several such predators were recognized (9-11). These predators occupied a primary level, but *Anomalocaris* also possessed at least the size and physical ability to exploit a secondary level.

Our excavations of 1990-92 at Chengjiang yielded fossils of giant predators of three different kinds, including complete specimens of *Anomalocaris* and a related form. *Anomalocaris* was initially described on the basis of isolated frontal appendages. These, the disassociated jaws, and a body found later were interpreted as three separate animals until such parts were found together in a nondisarticulated specimen from the Burgess Shale (12). However, this *Anomalocaris canadensis* specimen lacked the posterior part. A tapering, blunt body

J.-y. Chen and G.-q. Zhou, Nanjing Institute of Geology and Palaeontology, Academia Sinica, Chi-Ming-Ssu, Nanjing 210008, People's Republic of China.
L. Ramsköld, Museum of Palaeontology, University of Uppsala, Norbyvägen 22, S-752 36 Uppsala, Sweden.

*To whom correspondence should be addressed.